

ADDITIVELY MANUFACTURED INCONEL® ALLOY 718

Raymond C. Benn & Randy P. Salva

Materials and Process Engineering, Pratt & Whitney,
400 Main Street, E. Hartford, CT 06108

Keywords: Additive Manufacturing process/product, INCONEL® alloy 718

Abstract

Significant contributions have been made in recent years to the development of Additive Manufacturing (AM) technology. Improvements in laser and electron beam-based AM equipment using powder injection, powder bed or wire feed systems have benefited from advances in software programs to convert complex CAD models into Digitally Manufactured parts. Wider acceptance of AM technology in, for example the aerospace industry, is driven by meeting stringent quality, schedule and cost requirements. These factors, in addition to the specific property requirements and level of part-family complexity, strongly influence the selection of the appropriate Additive Manufacturing process. This presentation will briefly review some of the factors and criteria that must be addressed to transition an “AM opportunity” into a viable business case.

Introduction

Additive Manufacturing (AM) may be defined as: a collective term for manufacturing technologies, which in an automated process produce 3-D objects, as a whole or in part, directly from 3-D CAD data, by the successive addition of materials without the use of specialized tooling. AM is a relatively new technology with a history spanning ~40 years. This is insignificant compared to “Subtractive” and “Formative” shaping. However, significant contributions have been made in recent years to the development of AM technology and the state-of-the-art is rapidly changing. Improvements in laser and electron beam-based AM equipment using powder injection, powder bed or wire feed systems have benefited from advances in software programs to convert complex CAD models into Digitally Manufactured, i. e., “e-manufactured” parts.

Wider acceptance of AM technology use in, for example the aerospace industry, is driven by meeting stringent quality, schedule and cost requirements. These “business case” factors, in addition to the specific property requirements and level of part-family complexity, strongly influence the selection of the appropriate Additive Manufacturing process. Some AM processes are conducive to small, complex geometry, Free-Form-Fabrication (FFF) parts, having tight-tolerance Net-Shapes. Others, programmed via robotics/multi-axis machines, can span the part size range up to FFF larger parts or feature-additions. The surface finish on products from several AM processes is still Near-Net-Shape. An important goal is the minimization of any post-processing, such as machining or surface finishing, to achieve Net-Shape capability within the surface finish tolerances of the part design.

Experimental Methods and Results

There is a plethora of possible AM processes, materials, part quality standards and design property requirements. Hence, the down-selection methodology to transition an “AM opportunity” into a viable business case needs to be discerning in coverage and cost-effective. The metallurgical approach taken as part of the present work methodology was to define a standard shape, which could be manufactured by each AM process under consideration. The material of choice was INCONEL alloy 718, although 625 and Co-based alloys have also been evaluated. The standard shape was a 3.15 inch (80mm)-sided cube, which enabled X (run), Y (traverse), Z (build) and Z-interface orientations to be characterized and compared using ASTM approved specimens. The AM alloy 718 cubes from each process were evaluated for:

1. Microstructure and quality (porosity, inclusions etc.),
2. Mechanical properties (monotonic and time-dependent)
3. Shape-forming capability (surface finish and freeform fabrication).

Four relatively mature AM processes, were evaluated to down-select a suitable process that met structure/property/shape-forming and business case criteria for a given part family. The AM processes included Electron Beam Wire (Metal) Deposition (EBWD), Direct Metal Laser Sintering (DMLS), Laser Powder Deposition (LPD) and Gas Metal Arc Welding (GMAW). The EBWD process was evaluated in more detail and established (i) a methodology that was then adopted for the other AM processes, and (ii) a property data-base by which the other processes could be compared.

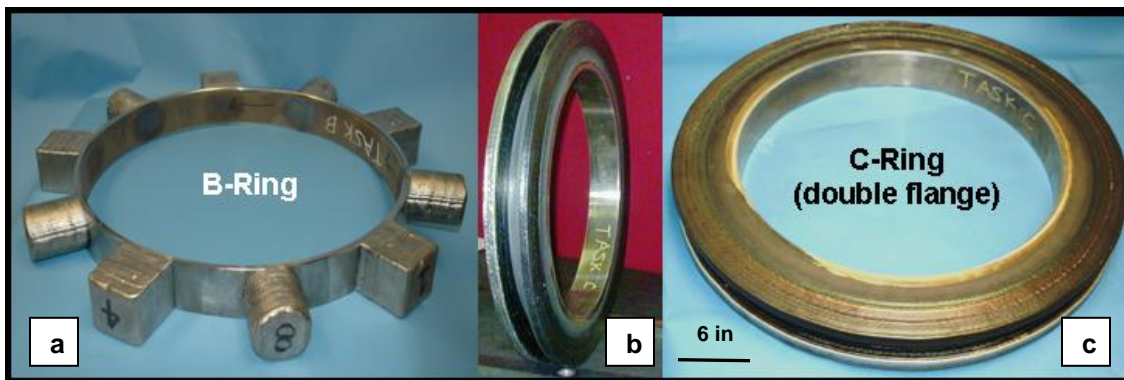


Figure 1. (a) B-Ring with EBWD-718 deposits. (b) C-Ring end-on with double flange deposits of EBWD-718. (c) C-Ring laid flat.

EBWD-718 Alloy Evaluation and Data-base Generation.

This AM process was studied earlier as part of the Materials Affordability Initiative [1]. In the present work EBWD-718 alloy was further characterized extensively, using the “add-on” cube methodology, to establish a “minimum design space” data-base for a given part. Figure 1 shows a typical test assembly of rolled AMS 5663 ring with EBWD cubes, cylinders and flanges, which simulate a generic structural case component. The rolled ring wall was thicker (~0.5 in.) than typical case walls; because the focus here was first to characterize the structure and mechanical properties of EBWD-718 deposits *per se* and the interfaces with wrought alloy 718 (AMS 5663). Figure 2 shows the progression

from deposit to test specimen orientation plan. All deposits were heat treated to the wrought alloy specification (AMS 5663) because the ring was the primary component, i.e., solution at 1750°F/1h followed by precipitation (aging) at 1325°F/8h + 1150°F/8h: (i.e. Solution Treat and Age: STA). Then, the EBWD data were compared with typical cast (e.g., AMS 5383) and wrought (AMS 5663) alloy 718, respectively. This data-base would, therefore be available when addressing the challenging manufacturability aspects of producing such casings with thinner walls, typical of actual parts.

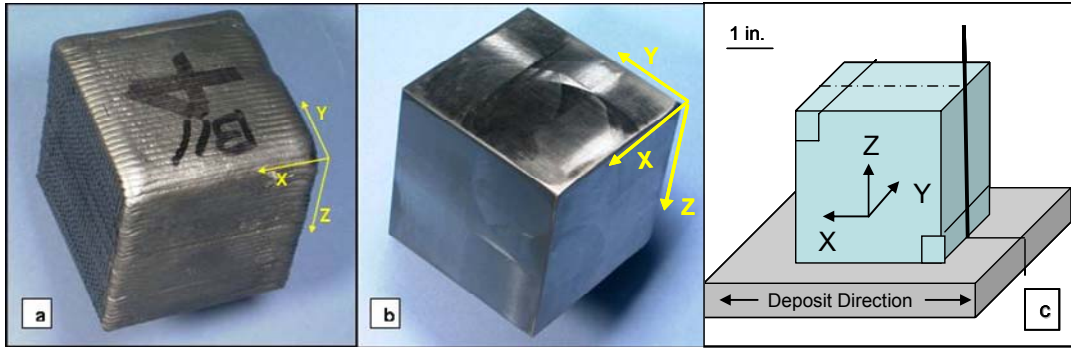


Figure 2. (a) As-deposited EBWD-718, (b) Machined cube, (c) Specimen orientations: X; run (deposit/scan/long. travel), Y; traverse (shape index/axial) and Z; build/radial.

The EBWD data-base included tensile, creep, notch-smooth stress rupture and, in particular, LCF matrices. Figure 3 is typical of the general trend observed in all these properties, when compared with cast and wrought 718 respectively. The average EBWD-718 properties were typically better than cast (AMS 5383 min.) and closer to wrought (AMS 5663 min.) alloy 718. The data represents the combined average of X, Y, Z and Z-interface orientations of the cubes.

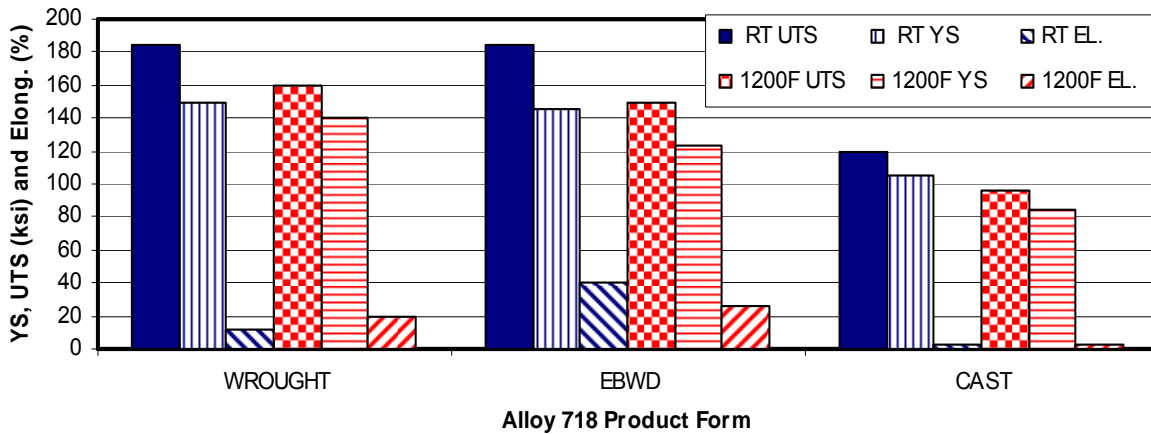


Figure 3. YS and UTS (average) properties of EBWD-718 vs. wrought (AMS 5663 min.) and cast (AMS 5383 min.) alloy 718.

However, directionality of the EBWD process leads to microstructural differences between orientations as indicated in Figure 4. These structural orientation differences combined with possible effects on porosity (under-bead, between passes and dissolved gas) can influence properties. Summarizing such effects in the present work on EBWD-

718; it was determined that the X- and Y- orientations had similar monotonic properties. The LCF properties of X- and Y- directions also fell within the same ranges and the minor differences between X- and slightly lower Z-direction properties did not appear significant. There was more scatter in the Z-interface properties, but overall, probability plots of the individual and/or combined LCF data followed log-normal distributions and indicated that the AM material orientations had little significant effect on LCF properties, as shown in Figure 5. Therefore, all the EBWD data from both X- and Z- orientations could be combined for performance analyses.

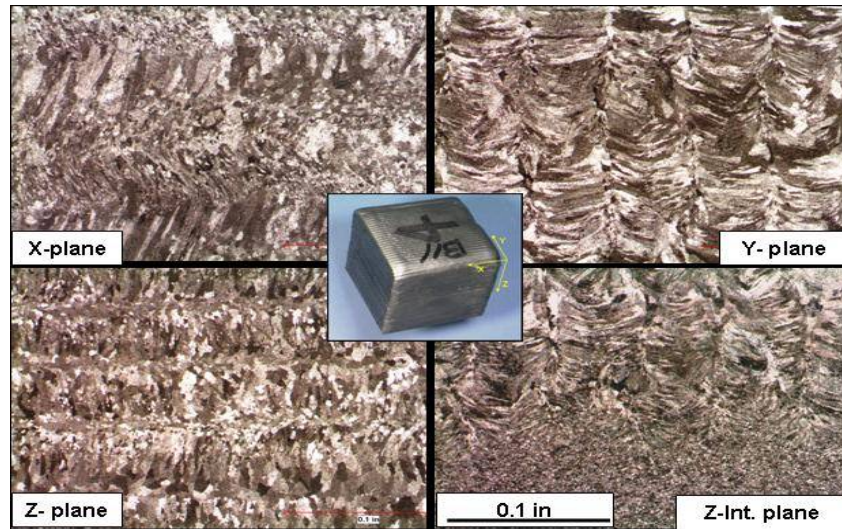


Figure 4. EBWD-718 cube macrostructures vs. deposition mode/test orientations (STA).

While this conclusion on orientation effects was derived for the EBWD data, it cannot be assumed for other AM processes having different AM modes, environments and controls. Orientation effects need to be characterized in reference to the AM process, component build geometry and respective Design Space property requirements. The EBWD-718 material was very clean, as expected from a high vacuum process, so that any inclusion-related orientation effects should be negligible. Microstructural grain shape and size differences between orientations would have more effect on properties.

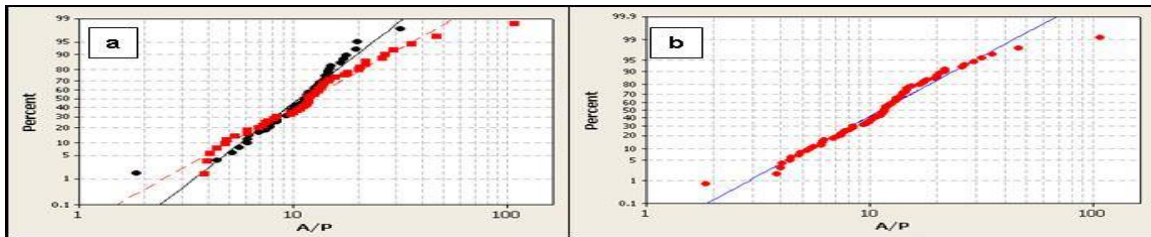


Figure 5. Log-normal Actual/Predicted LCF distribution for (a) orientation X (red squares) and Z (black circles) data and (b) combined X and Z data.

As layers are deposited, re-melting of underlying layers occurs and the root of the weld deposit may penetrate through one or more layers dependent on the level of heat input

from the electron beam. Figure 6 shows some delineation between weld layers via interface areas of re-melting and nucleation of fine grains. Figure 6(a) illustrates the re-melting and grain boundary formation through previous deposits, whereas 6(b) is a montage showing both weld-on-weld deposits and weld deposit penetration into the interface with AMS 5663 substrate plate. Normal grain boundary and intra-granular precipitation of delta needles are seen in the deposits after subsequent STA.

GMAW, LPD and DMLS Evaluations Compared to EBWD.

The EBWD-718 data-base was then used as a "yard-stick" to compare/contrast AM products in the same form (i.e., ~3 inch cubes) from the four processes; EBWD, DMLS, LPD and GMAW. The scope was broadened to include second vendor sources for LPD (i.e., LPD-1 vs. LPD-2) and DMLS (i.e., DMLS-1 vs. DMLS-2) cubes. The metal deposition speeds used for each AM process were the nominal rates selected by each vendor, based on their respective experience. The effects of increased deposition speed were also investigated for LPD (i.e., LPD-1 vs. LPD-1a). None of the four AM process products were Hot Isostatically Pressed (HIP'ed); the objective being to evaluate "as-deposited (i.e., as-sintered for DMLS) and HT'ed" alloys equally, without any possible HIP benefits to their properties.

1. Structure and Quality Screening. Fluid Penetrant Imaging (FPI) and X-ray measurements were made on machined, orthogonal sections of the cubes; primarily to identify any significant defects. Other than some sub-surface porosity indications in some AM process cubes, the overall bulk soundness was acceptable. These techniques did not have the optical resolution to detect any fine pores conclusively. Density measurements and Image Analyses were made on many small sections of the as-deposited material. These sections were then heat treated at 2175°F/2h and re-examined for any Thermally Induced Porosity (TIP). Figure 7 compares the density measurements made on precision machined blocks from each of the different process products and alloys. The % density difference ($\Delta\rho$) between as-deposited and TIP is shown as the open rectangles from the dashed, zero % difference line.

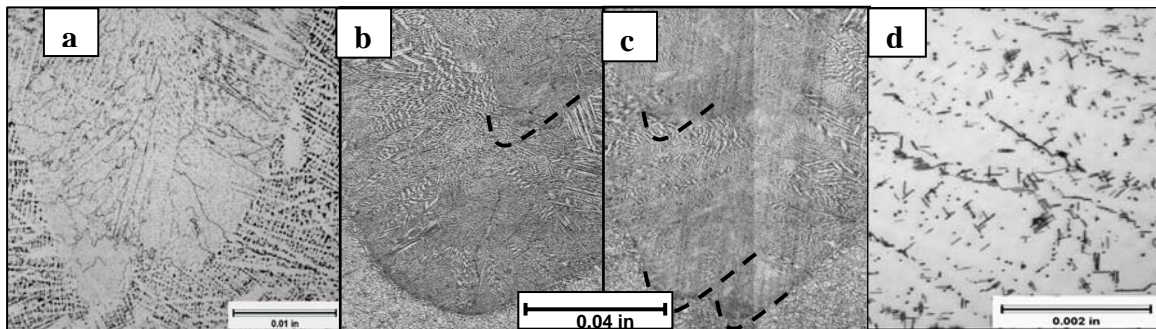


Figure 6. (a) Micrograph showing re-melting and grain boundary formation at the root of the overlaid EBWD-718 pass. (b, c) Montage showing weld-to-weld (dashed line) and weld-interface deposit penetration and (d) Precipitation of grain boundary and intra-granular delta (δ) phase after STA.

All the alloy-718 products had, essentially, the same bulk density i.e. 8.20-8.25 g/cc (0.296-0.298 lb/cubic inch), but the density change with TIP increased in the ascending order; DMLS-1, EBWD, GMAW, LPD-1, LPD-2 and LPD-1a. In the LPD process trials, increased powder deposition speed (e.g., a ~2-fold speed increase from LPD-1 to LPD-1a) was found to increase $\Delta\rho$ and there was some variation between vendors (LPD-1 vs. LPD-2). In other AM alloys such as DMLS-625 and DMLS-CoCr, there was negligible $\Delta\rho$ and also little difference in $\Delta\rho$ between different DMLS-CoCr vendors (DMLS-1 vs. DMLS-2, under -CoCr in Figure 7).

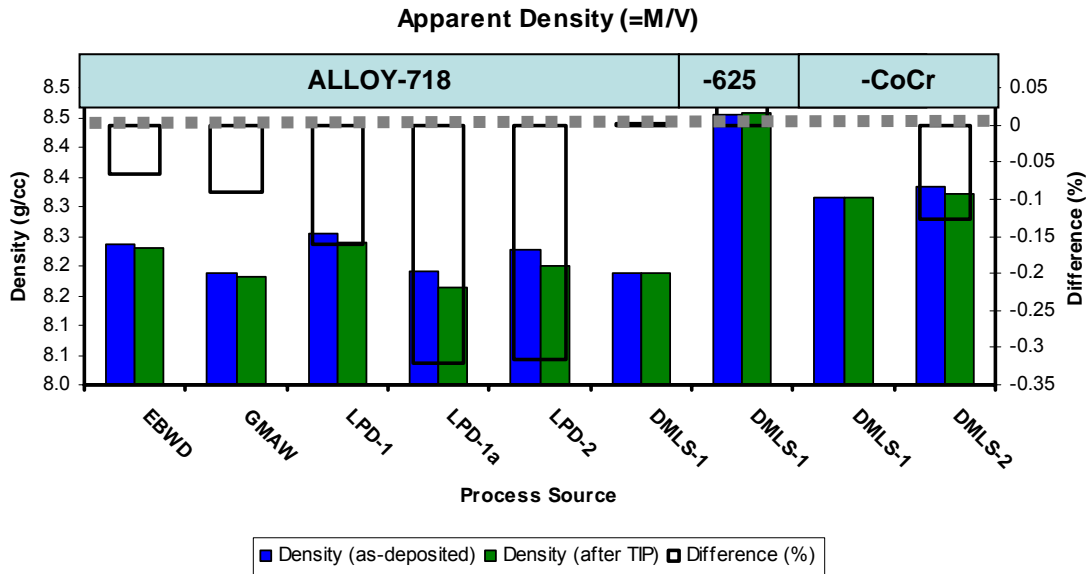


Figure 7. Apparent density (=M/V) variation between different AM process products.

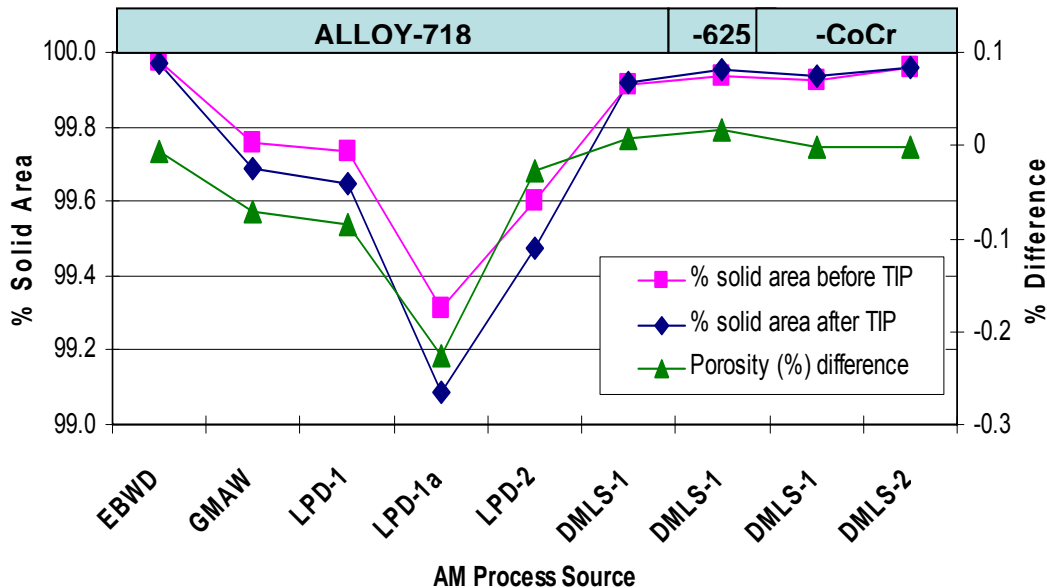


Figure 8. Image Analysis porosity variation between different AM process products.

There was good correlation between the measured density and the actual porosity, as determined from multiple image analyses of cube sections in both polished and lightly

etched conditions. Figure 8 compares the same products but indicates that the bulk solid% of DMLS and EBWD were both ~100% and the GMAW was 99.8% dense before and after TIP. The LPD process products were ~99.7% dense, falling to ~99.2% with increased deposition rate. The purpose of these studies was to quantify the amount of bulk porosity, typically observed as spherical pores, and relate it to any effects on mechanical properties, in particular, the time-dependent behavior.

Similar to the EBWD studies, the other AM products were also microstructurally characterized to compare and contrast possible effects on performance. Figure 9 shows that the as-deposited Y-plane microstructures of (a) GMAW and (b) LPD show less penetration into the substrate than EBWD, partly due to lower heat-inputs. The GMAW technology used was a MIG “dip-arc” process with digitally-controlled drop detachment from the wire, which reduces the heat transfer into the weld. The LPD also had lower heat transfer, but higher porosity than the other AM processes as indicated in Figures 7-8 and revealed in Figure 9 (b) as black spheres (e.g. circled) indicative of gas porosity.

Aside from operating parameters, the porosity content, size/shape and oxygen content of the powder are important considerations in superalloy powder-based AM processes. The powder mesh size and source process, e.g., conventional gas vs. rotary atomized vs. plasma rotating electrode process (PREP) can, for example, influence the amount of hollow particles obtained. Typically, fine (-200 mesh or less) conventionally gas atomized powder results in lower porosity than coarse powder [2]. Rotary atomized

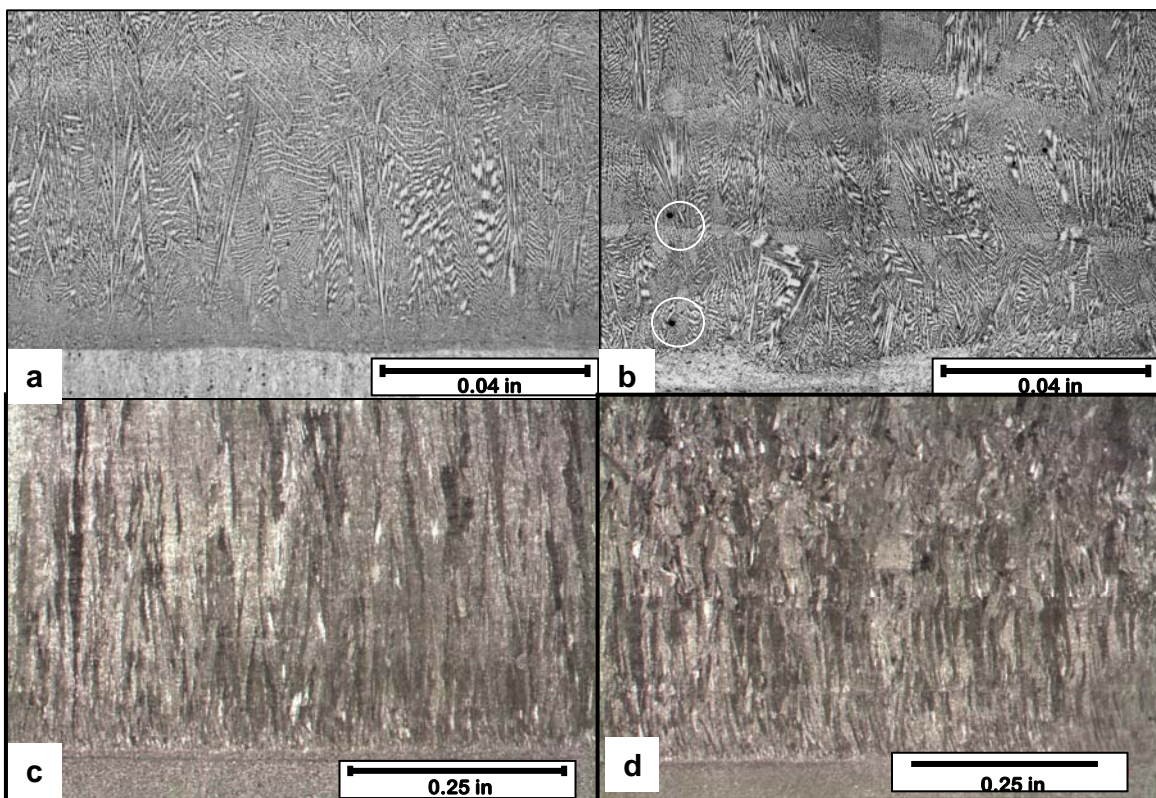


Figure 9. Alloy 718 as-deposited microstructures of (a) GMAW, (b) LPD (montage) and macrostructures of LPD at (c) nominal and (d) 2x nominal deposition speed.

powder and PREP powder [2, 3] result in progressively lower porosity contents. Finer powders tend to have higher oxygen contents. It is recognized that different AM powder process vendors and users may have different powder preferences depending on cost and the product integrity requirements.

A directional grain structure, illustrated in Figures 9 (c-d), appears to also differentiate the LPD from other AM processes. The directional solidification is characteristic of a planar solidification front associated with high G/R (temperature Gradient/solidification Rate) values in line with conventional solidification theory. The primary process variables are energy and mass input, which are controlled by laser (or EB) power, deposition speed and powder (or wire) feed [4]. These variables influence the melt pool size, shape and solidification rate, which directly affects the microstructure. The absorbed power dominates, but Figure 9(d) indicates that doubling the deposition speed can also move the G/R ratio into melt solidification conditions that nucleate equiaxed grain shapes.

The directional structures with any preferred orientation, typically lead to anisotropic mechanical properties [4-6], which may be beneficial for high temperature creep strength at the cost of lower transverse ductility. If the melt pool solidification and alloy feed parameters could be controlled sufficiently; the microstructure and/or the alloy could be tailored to suit the component property requirements. This effect could, in general, be achieved for LPD and related AM processes. An ultimate goal in AM is to closely monitor applicable melting and structural solidification parameters continuously, with anticipative closed-loop feed-back control, in real time to prevent potential defects in the product.

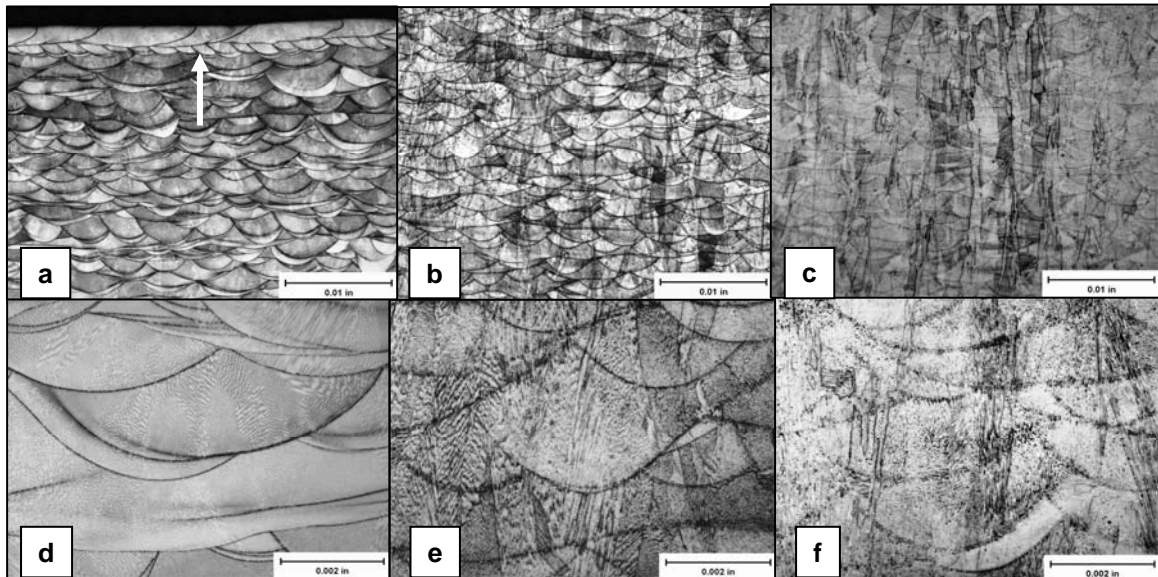


Figure 10. “As-deposited” (as-sintered) DMLS structures of CoCr alloy (a, d), Alloy 718 (b, e) and Alloy 625 (c, f).

The structure of the sintered DMLS layers also differentiates this “powder bed” AM process product from the preceding “deposition” AM technologies. In general, the rapidly solidified DMLS structures are finer, as shown in Figure 10. Examples of DMLS-CoCr and DMLS-625 solid solution alloys are included for comparison of the internal structure content with DMLS-718. The increasing alloy content is somewhat reflected in the sintered deposits; with the high content of precipitation hardening elements in alloy 718 leading to a greater response in microstructural etching.

In powder-bed AM processes, the energy beam “spot” (laser or EB) fuses metal powder particles *in situ* via surface sintering in a localized melt pool; whereas powder (wire)-deposition processes feed alloy into a melt pool. The melting mode and resultant solidification rate can, therefore, contribute to and differentiate between the structural characteristics. Figure 10(a) is an example of “build mode” wherein the outside surface perimeter is first defined by the laser forming a parallel line of smooth, elongated melts (arrowed). The bulk interior is then “filled in” via laser sintering rasters, which should be contiguous with the perimeter wall to make a solid transition and avoid leaving sub-surface porosity at discontinuities.

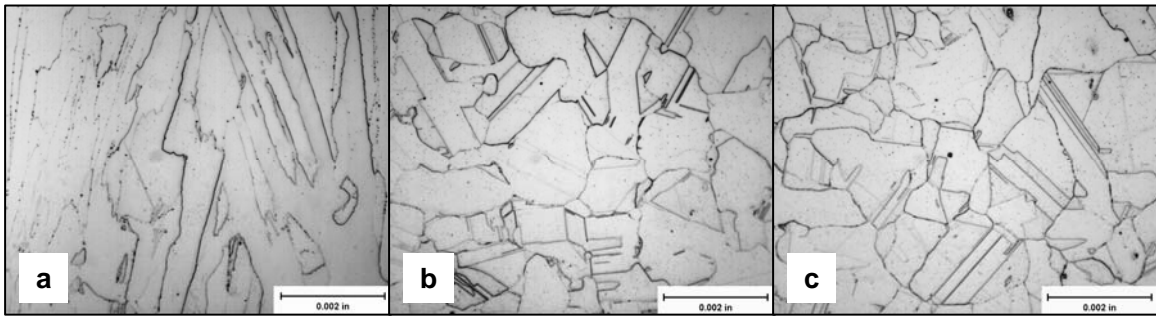


Figure 11. Effect of temperature on recrystallization and grain growth response of “as-sintered” DMLS-625; (a) 1800°F/1h, (b) 2000°F/1h and (c) 2100°F/1h.

Fine dendritic structures are visible inside the “beads” and, similar to powder/wire feed systems, there appears to be some epitaxiality leading to “grain” structures across layers of beads. However, unlike LPD directional grains (Figure 9c), the DMLS “grain” shapes are discreet and irregularly elongated. As-sintered, the DMLS products, similar to other AM processes reviewed here, have internal stress levels that need to be relieved by heat treatment. Combined with the intrinsic energy of the high “grain boundary” area of the DMLS solids, the residual stress can drive recrystallization during Stress-Relief (SR) and/or Solution HT. Figure 11 indicates that the “bead” structure in as-sintered DMLS-625 (Figure 10f) is solutioned but jagged, roughly aligned and partially recrystallized grains remain at ~1800°F. Fully recrystallized, equiaxed grains are formed at 2000°F/1h (ASTM ~6 and ALA 4) with little grain growth at either 2100°F/1h or 2100°F/2h.

Precipitation hardenable alloy 718, similar to the solid solution alloy 625, shows the same temperature effect on grain shape during recrystallization. But, when as-sintered DMLS-718 is given the conventional solution heat treatment (SHT) at 1750°F/1h, followed by

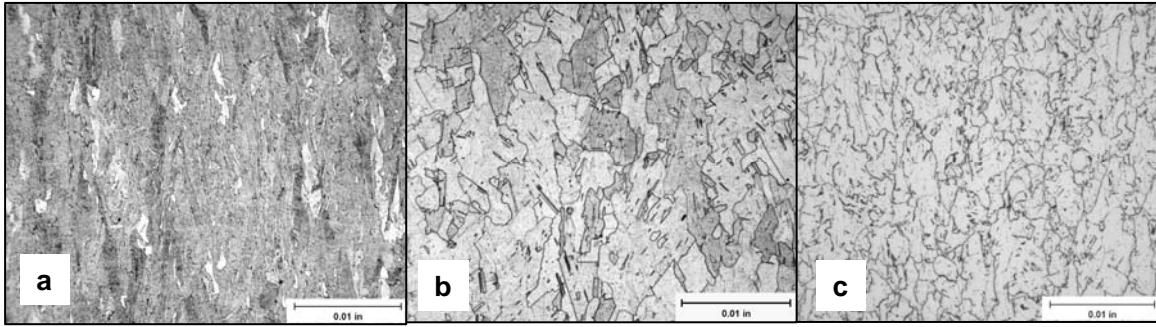


Figure 12. Effect of Stress Relief/SHT temperature +/- STA on recrystallization response of as-sintered DMLS-718; (a) 1750°F/1h + STA, (b) 2100°F/1h SHT and (c) 2100°F/1h + STA.

the standard AMS 5663 precipitation (aging) heat treatment (1325°F/8h + 1150°F/8h); the microstructural complexity is revealed, (Figure 12a), and is ostensibly reminiscent of a worked product. Re-solutioning as-sintered solid alloy at higher temperatures, then rapid cooling, produces equiaxed grains. Figure 12(b) shows an equiaxed, twinned microstructure (ASTM~5) given a “homogenization” heat treatment. Homogenization of conventional (cast) alloy 718 is typically performed at 2000°F/1h to dissolve Laves phase. Surprisingly, insufficient recrystallization was observed even at 1950-2000°F. So 2100°F/1h was adopted in the present work simply to compare with alloy 625 shown in Figure 10(c); recognizing that delta phase also re-solutions above its solvus (~1850°F) When given the full “homogenization + Solution Treat and Age (STA),” the more detailed microstructure shown in Figure 12(c), was developed.

This microstructure was, subsequently, analyzed in detail. The optical micrograph features, circled in Figure 13(b), were characterized via SEM and EDS spectra. Grain boundary and intra-granular δ needles were prevalent and a minor amount of Laves phase was retained, despite the high temperature homogenization treatment. Nb/Mo-rich MC carbides were identified at grain boundaries and, in particular, as “prior particle boundaries (ppb’s);” Figure 13(f). Evidence of these ppb’s was first observed in the recrystallization studies of alloys 625 (Figure 11a) and 718 (Figures 12c and circled in Figure 13b). The ppb’s were much less evident in the fully recrystallized alloy 625, but persisted in the recrystallized alloy 718. In general, the presence of significant ppb’s, in superalloy powder metallurgy products, can lead to intergranular cracking, low ductility issues and merits further discussion in relation to properties and recrystallization.

The origin of ppb’s is typically attributed to the presence of fine, stable oxides (Al_2O_3 and TiO_2) on the powder particle surface, which may nucleate MC precipitation [6]. Alloy 718, with higher Al, Ti and Nb content than alloy 625, would be more prone to form ppb’s; whereas CoCr and 304 SS, with no such “oxygen-getters” are not prone to ppb’s.

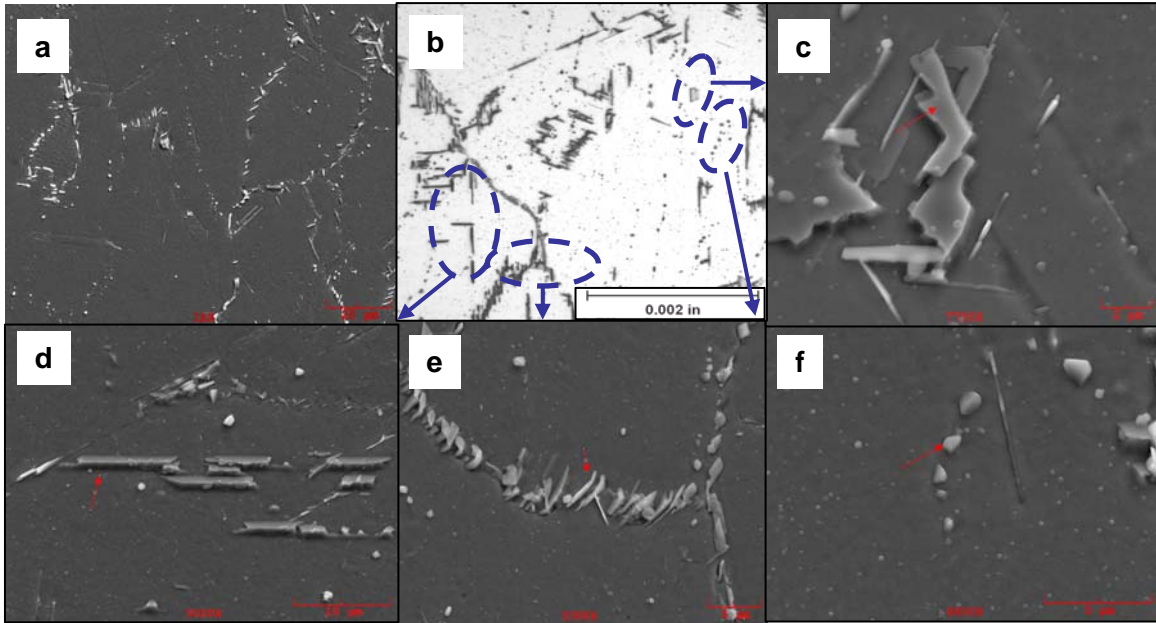


Figure 13. SEM evaluation selected optical features (b) of DMLS-718, (Homogenized + STA). (a) General structure, (c) Laves phase, (d) Intra-granular δ phase needles, (e) Fine grain-boundary δ needles and MC carbides, (f) prior particle grain boundary (ppb) MC carbides.

In general for all superalloy powder-deposition or powder-bed AM processes, the oxygen content of the as-used powder, deposition/sintering atmosphere and subsequent HT processing should, therefore, all be controlled as low as possible to minimize oxide and MC formation in the form of ppb's. Preferably, the high purity argon atmosphere should have less than 10ppm oxygen. Once formed, the effect of the ppb's, e.g. NbC, can be reduced by high temperature HT's, e.g., SHT and/or HIP (hot-working *per se* is not an option for net-shape), to re-solution and/or break-up the networks, followed by cooling at fast enough rates to reduce the diffusion rates of Al, Ti and C to the grain boundaries and minimize reformation of more MC carbides. Such high HT's can cause excessive grain growth, so it is important to simply prevent any ppb formation. In addition, the recrystallization and grain growth could be impeded by ppb networks and may explain why higher than expected temperatures were required to SR/SHT the present DMLS-718.

2. Mechanical Property Screening. An abbreviated comparator test matrix was developed, based on the more comprehensive data-base developed for EBWD-718. The as-deposited GMAW, LPD and DMLS stock of ~3" cubes were processed identically to the EBWD material. The same types of testing were performed, i.e., tensile, Notch-Smooth stress rupture, Smooth LCF and Notched LCF but, in lieu of a range of selected temperatures, spot checks at 1200°F were run for tensile/stress rupture and at 800°F for LCF tests. Orientation effects were also studied at these conditions and compared with the EBWD-718 data-base.

The comparison of 1200°F tensile properties from each of these AM processes indicated similar trends to EBWD in that X- and Z-orientation data were not significantly different

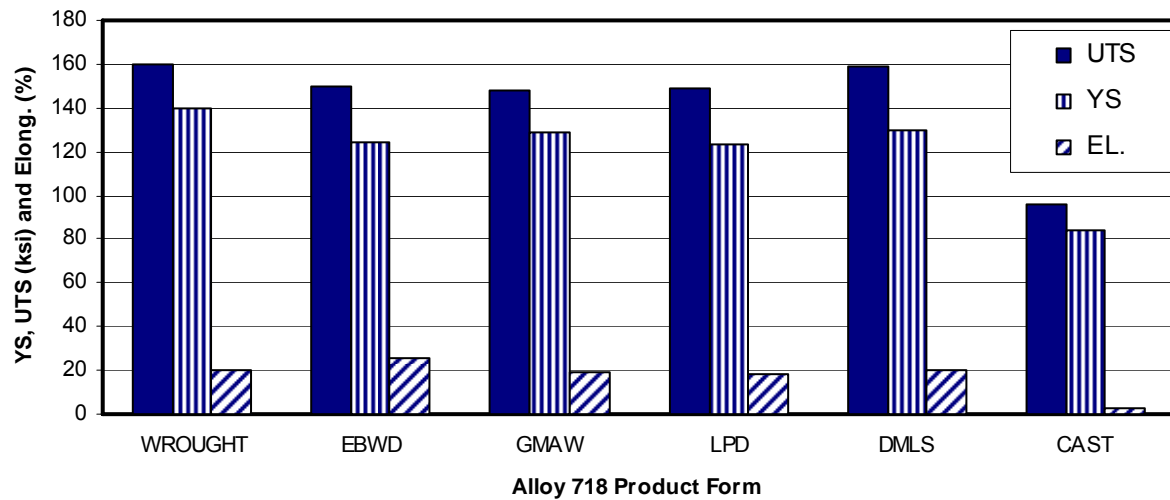


Figure 14. YS, UTS and Elong. (1200°F average) properties of alloy 718 product from various AM processes, versus wrought (AMS 5663 min.) and cast (AMS 5383 min.).

so that average values are shown in Figure 14. The finer grain sizes in wrought and DMLS alloy 718, compared to the other AM processes, probably accounts for their slightly higher strength values.

In 1200°F/85 ksi, Notch-Smooth stress rupture tests, all the EBWD life data were close to wrought properties, with X- slightly higher than Z-orientation, and no indications of notch-sensitivity. The GMAW-718 behavior was similar, but with slightly lower overall lives than EBWD. However, in the DMLS-718 the Z-orientation lives were similar to EBWD but the DMLS X-orientation lives, similar to LPD X- and Z-lives, were lower. Unlike EBWD, in the DMLS system the Z- (or Build) orientation appears to give better properties. The difference in relative Z-orientation properties may be related to the difference in AM mode between powder or wire deposition, versus powder-bed sintering solidification.

Both DMLS and LPD-718 alloy showed some notch-sensitivity which, assuming a satisfactory disposition of grain boundary δ phase needles (evident in Figure 13e), could be attributed to some ppb effects in the DMLS and porosity in the LPD product respectively, observed earlier. Powder/process control optimization should remedy both.

The fatigue lives of DMLS- and LPD-718 tests fell within the lower end of the EBWD scatter-band data for both SLCF (800°F/R = 0.05) and NLCF (800°F/R = 0.05/Kt = 2.18) cross-check tests. However, some premature failures were obtained with GMAW-718 which were subsequently attributed to Al oxide inclusions identified at the crack nucleation sites in SEM/EDS analyses of the fractures. The presence of these inclusions was attributed to inadequate inert gas (argon) shielding during GMAW, which lead to areas of deposit oxidation. Again, process control optimization should remedy this.

In general, all the AM process test data and performance were better than Cast-718 under the same conditions, but lower than EBWD-718, which in turn were closer to Wrought-718 properties. Plausible reasons are proposed above for selected property departures from the EBWD-718 data-base, related to microstructural differences including porosity and oxygen control/oxide related effects on “feed-stock” and process parameters.

3. Screening of Shape-Forming Capabilities. The third criterion to screen the selected AM Processes was essentially the Free-Form-Fabrication (FFF) capability. The EBWD, GMAW, LPD and DMLS Additive Manufacturing processes are currently at different levels of shape and dimensional tolerance control. The differences are due to intrinsic operating parameters, such as “spot” resolution and the control (including feed-back) designed into the software programming. For “Add-on” features and FFF wire/powder deposition capability using EBWD, GMAW or LPD the multi-axis programming of the deposition head influences shape capability and part size is only limited, essentially, by atmosphere (vacuum or inert gas) control volume. Powder-bed processes, such as DMLS with a Laser energy source and EBM (Electron Beam Melting, ARCAM [7]) with an EB energy source, benefit from the established SLA/SLS/EBM-type technologies, which have tighter tolerance control favoring very complex parts produced within the powder bed volume limits.

The ~3” cube used in the current work, provided a good measure of the shape-forming and dimensional tolerance capabilities of the different AM processes. The cubes were each produced at the nominal deposition rate then used by each vendor. These rates differ according to the type of process, but are generally assumed optimum for the vendors’ products at the time of procurement. It has been demonstrated in the current work that faster rates are not necessarily better if they result in loss of integrity/dimensional control.

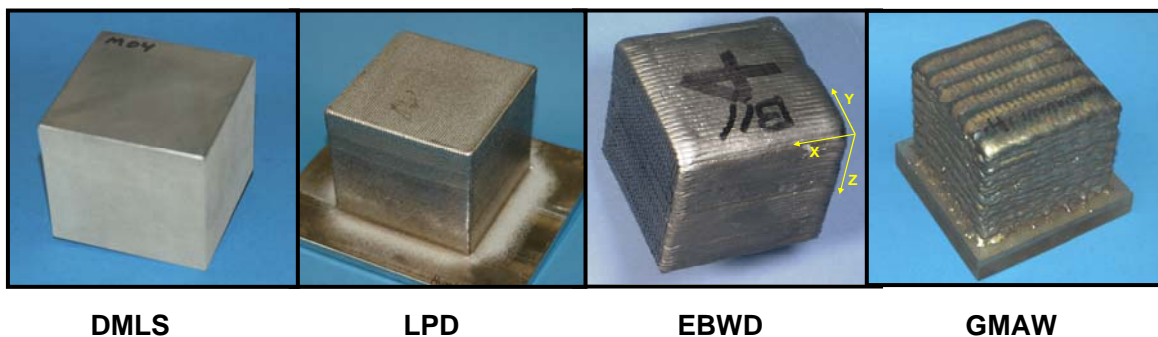


Figure 15. Shape-forming capability of selected AM processes; as indicated by simple cube samples.

The shape-forming characteristics were gauged via surface roughness/integrity and CAD-forming capabilities. Based on these cubes, Figure 15 shows that the level of shape definition decreases in the order; DMLS > LPD > EBMD > GMAW. The blocks represent a guide that is confirmed by actual products. DMLS with a superior profile tolerance of ± 0.005 – 0.010 met the criteria for best complex shape-forming capability.

Discussion

The screening results, albeit a limited overview, enabled the AM processes/products to be compared, contrasted and also highlighted some areas for further development. Given this metallurgical overview, the process of sequestering the appropriate AM process/product for a specific gas turbine part requires consideration of other technology drivers including performance, quality, schedule and cost.

Manufacturability. The benefits of meeting these technology drivers can only be realized if the selected AM process/product has acceptable “manufacturability.” From experience, failure to meet this criterion is often the downfall of new process/products. Some, essentially non-metallurgical, guidelines for AM include:

- Reduced Buy-to-Fly ratio.
- Manufacture (OEM) and/or repair.
- Initially use “work-horse” alloys such as alloy 625, 718 and Ti-6-4.
- Low to medium production quantity component.
- Low to medium risk component, e. g., static structures first.
- Defer initially from large thin-wall components.
- Prefer stand-alone components over assembly sub-components.
- Relevant data-base and manufacturing experience.
- Supplier qualification, source approval and monitoring.
- Process/product must be robust, repeatable and recorded.

Development of closed-loop, feed-back control of the melt-pool during alloy “addition,” to automate the AM process in real-time, can provide some fidelity to manufacturing. It is an active area for modeling and experimental research [4, 8].

Company Acceptance. Typically, each OEM will need to review the field and evaluate several AM process/products to determine the capabilities, limitations and build the high level of confidence required for company acceptance. Introduction of a relatively new process such as AM, even using familiar alloys such as 718, requires that properties be characterized against internal design data-bases because the product behavior is a function of process, heat treatment, chemistry and orientation.

The requirements on performance and quality are much more stringent for aerospace superalloys compared to general engineering alloy applications. Cost-benefit analyses must justify the investment [1] and the levels of “production pull” and risk are key determinants in any business case decisions. Internal specifications on AM materials and/or processes need to be developed and rationalized to simplify number and content. Engineering Standard Work should be established incorporating a “Design for AM.” This approach would guide the designer to capitalize on the unique features that AM offers in producing parts with very short lead-times that are difficult, labor-process intensive or, even, impossible to manufacture using conventional methods.

Industry Acceptance. Overall, for industry-wide acceptance of AM, unified AMS/ASTM Specifications [1] and Standards are needed for conformity, repeatability and risk-reduction within and between different companies. ASTM has established Committee

F42 on Additive Manufacturing Technologies [9], which is developing Standards through several sub-committees addressing specific segments, respectively.

Conclusions

1. The cost, scale, level of part-family complexity and process/product metallurgical factors strongly influence the selection of the appropriate Additive Manufacturing option; all must be considered to transition an “AM opportunity,” into a viable business case.
2. The metallurgical approach of manufacturing a standard test cube provided a simple methodology by which AM process/products could be evaluated, compared and screened for a given part.
3. In general, Z-orientation (build) properties were slightly lower than X(Y) for deposition AM processes (EBWD, LPD and GMAW), but slightly higher for DMLS (powder bed sintering). The EBWD-718 product quality was particularly high with close to wrought properties and little significant orientation effects on performance analyses.
4. The AM processes are currently at different levels of shape and dimensional control due to intrinsic operating parameters associated with the localized melt control and solidification. In this investigation, the level of shape definition decreased in the order; DMLS>LPD>EBMD>GMAW.
5. Company and industry adoption of AM requires the above rigor and unified AMS/ASTM Specifications and Standards for conformity, repeatability and risk-reduction within and between different companies.

References

1. A. Debicari, et al., MAI Consortium on “Additive Manufacturing for Superalloys – Producibility and Cost Validation,” Final Report, CA No. F33615-99-2-5215, March 6th, 2009).
2. H. Qui, M. Azer and A. Ritter, “Studies of standard heat treatment effects on microstructure and mechanical properties of laser net shape manufactured INCONEL 718,” *Metallurgical and Materials Trans. A*, 40A, October 2009, 2410-2422.
3. X. Zhao et al., “Study on microstructure and mechanical properties of laser rapid forming INCONEL 718,” *Materials Science and Engineering A*, vol. 478, 2008, 119-124.
4. R. J. Moat, A.J. Pinkerton et al., “Crystallographic texture and microstructure of pulsed diode laser-deposited Waspaloy,” *Acta Materiala*, 57 2009, 1220-1229.
5. P. L. Blackwell, “The mechanical and Microstructural characteristics of laser-deposited IN718,” *Journal of Materials Processing Technology*, vol. 170, 2005, 240-246.
6. G. A. Rao et al., “Influence of modified processing on structure and properties of hot isostatically pressed superalloy Inconel 718,” *Materials Science and Engineering*, vol. 418 No.1-2, 2006, 282-291.
7. www.arcam.com
8. R. Scudamore., TWI private communication, Oct 2008.
9. “Additive Manufacturing Technologies,” Committee F42, ASTM International, www.astm.org.